Contrasting effects of aeration on methane (CH_4) and nitrous oxide (N_2O) emissions from subtropical aquaculture ponds and implications for global warming mitigation

Ping Yang[a,b*], Kam W. Tang[c], Hong Yang[d,e], Chuan Tong[a,b], Linhai Zhang[a,b], Derrick Y. F. Lai[f], Yan Hong[a,b], Lishan Tan[f], Wanyi Zhu[a,b], Chen Tang[a,b]

[a]*School of Geographical Sciences, Fujian Normal University, Fuzhou 350007, P.R. China*

[b]*Key Laboratory of Humid Subtropical Eco-geographical Process of Ministry of Education, Fujian Normal University, Fuzhou 350007, P.R. China*

[c]*Department of Biosciences, Swansea University, Swansea SA2 8PP, U. K.*

[d]*Department of Geography and Environmental Science, University of Reading, Reading, UK*

[e]*College of Environmental Science and Engineering, Fujian Normal University, Fuzhou, 350007, China*

[f]*Department of Geography and Resource Management, The Chinese University of Hong Kong, Hong Kong, China*

***Correspondence to:**

Ping Yang (yangping528@sina.cn)

Telephone: 086-0591-87445659 Fax: 086-0591-83465397

ABSTRACT

The increasing number of small-hold aquaculture ponds for food production globally has raised concerns of their emission of greenhouse gases (GHGs) such as methane (CH_4) and nitrous oxide (N_2O). Aeration is commonly applied to improve oxygen supply for the farmed animals, but it could have opposite effects on GHG emission: It may inhibit anaerobic microbial processes that produce GHGs; it may also increase water-to-air GHG exchange via physical agitation. To resolve the overall effect of aeration on GHG emissions, this study analyzed and compared the monthly CH_4 and N_2O emissions from earthen shrimp ponds with and without aeration, in the farming period for two consecutive years, in an estuary in subtropical southeastern China. CH_4 flux was mainly influenced by water temperature and dissolved oxygen, and it was significantly higher in non-aerated pond (7.6 mg m^{-2} h^{-1}) than in aerated ponds (4.5 mg m^{-2} h^{-1}), with ebullition accounting for >90% of the emission. Conversely, non-aerated pond had ca. 50% lower N_2O flux than aerated ponds, and dissolved nitrate was the main driving factor. The combined CO_2-equivalent emission in aerated ponds (avg. 10,829 kg CO_2-eq ha^{-1} yr^{-1}) was substantially lower than that in non-aerated pond (avg. 17,627 kg CO_2-eq ha^{-1} yr^{-1}). While aeration may increase diffusive flux of GHGs via physical agitation, it remains a simple and effective management practice to decrease the overall climate impact of aquaculture ponds.

Keywords: Artificial aeration; Greenhouse gases (GHGs) emission; Sustained-flux global warming potential (SGWP); Climate mitigation; Aquaculture pond

1. Introduction

The increasing number of aquaculture ponds for food production worldwide (FAO, 2017) causes great concerns of their climate impact through emissions of greenhouse gases, for example, methane (CH_4) and nitrous oxide (N_2O) (Grinham et al., 2018; MacLeod et al., 2020; Yuan et al., 2021). Williams and Crutzen (2010) estimated that the aquaculture sector contributed 0.09 Tg or 0.3% of the global anthropogenic N_2O emission in 2008. The annual global N_2O emission from aquaculture is projected to increase to 0.6 Tg by 2030, or 5.7% of anthropogenic N_2O emission (Hu et al., 2012). Based on worldwide database of freshwater aquaculture, it was estimated that the top 21 aquaculture producers emitted 6.0±1.2 Tg CH_4 and 36.7±6.1 Gg N_2O in 2014 alone, which were equivalent to 1.8% and 0.3% of global anthropogenic CH_4 and N_2O emissions, respectively (Yuan et al., 2019).

In China, the total area for aquaculture pond has expanded to approximately 3.2×10^4 km^2 in 2018 (BFMA, 2019). Being the world's largest producer of aquatic products, around 60% (approximately 15,600 km^2) of China's aquaculture ponds are located along the coast (Duan et al., 2020). One of the main aquaculture operations in China is shrimp farming in small coastal ponds (with a total area of 2.4×10^3 km^2) (BFM A, 2019), which contributes approximately 12% of the global shrimp culture by areal coverage. Most shrimp ponds are maintained through feeds and aeration every day (Yang et al., 2017; Yang et al., 2020a; Chen et al., 2016), but some ponds are not aerated or with low aeration frequency. Although some efforts have been made to characterize the effect of feeds on greenhouse gas (GHG) production in aquaculture systems (Adegbeye et al., 2019; Chen et al., 2016; Soares and Henry-Silva, 2019; Yang et al., 2020b; Zhao et al., 2021), the effect of aeration is less clear, especially for small aquaculture ponds that are often not monitored properly (Kosten et al., 2020). A meta-analysis has shown that small aquaculture ponds tended to emit far more CH_4 than industrial-scale systems with proper aeration, and therefore wider use of aeration is recommended to mitigate CH_4 emission from aquaculture (Yuan et al., 2019). However, while aeration is expected to inhibit the anaerobic microbial processes that produce CH_4, it could also accelerate the water-to-air gas diffusive fluxes (Hu et al., 2013; Kosten et al., 2020). The balance between the two opposite effects would determine how aeration affects the net GHG emissions and global warming contribution of aquaculture ponds.

In order to improve our understanding of aeration effects on GHG emissions from aquaculture ponds, we analyzed and compared CH_4 and N_2O fluxes and their main driving factors, between aerated and non-aerated shrimp ponds over the farming period for two consecutive years in southeastern China.

2. Materials and methods

2.1. Research area

The research was carried out in earthen shrimp ponds (*Penaeus vannamei*) in the Shanyutan Wetland of the Min River Estuary (MRE) in southeastern China (Figure 1). The annual mean air temperature in the region is 19.6 °C and the mean rainfall is 1,350 mm (Tong et al., 2012). The average salinity is 4.2±2.5 ppt and the average range of semidiurnal tidal is 0.1–1.5 m (Tong et al., 2018). The dominant vegetation species include native *Phragmites australis* and *Cyperus malaccensis*, and the invasive *Spartina alterniflora*. Covering approximately 30% the Shanyutan Wetland, these shallow aquaculture ponds were created by removing the original marsh vegetation and converting bunds into steep slopes. The interval between the removal of native vegetation and the creation of pond was around 10–15 days.

2.2. Shrimp pond system and experimental design

The farming period was between May and November, producing a single crop annually. Before shrimp culturing, the ponds were filled to 1.5 ± 0.2 m deep with brackish water (salinity 4.2 ± 0.3) drawn from the adjacent estuary. Commercial feed pellets were added once in the morning (07:00) and once in the afternoon (16:00). Some of the ponds had aerators to oxygenate the water, but some ponds were not aerated. After harvesting in late November, water was discharged via spillways. Please refer to Yang et al. (2017; 2021) for more details of the aquaculture pond operation.

Water and gas samples were collected from one non-aerated pond (NAP) and two aerated ponds (AP I and AP II). The sizes of these three ponds ranged from 1.25 to 1.40 ha; water depth varied from 1.3 to 1.6 m. For the AP, aeration was provided by six 1,500-W paddlewheel aerators that ran almost continuously (stopped for a short time during the feeding periods). In each pond, a wooden bridge (approximately15 m long) extending from bank to center was used to collect samples at three locations: one near the bank, one in the mid-section of the bridge, and one at the pond center. Field sampling was conducted during the farming period, every month between June and November, for two consecutive years (2019 and 2020) for a total of 12 sampling campaigns in each pond. On each sampling day, all samples were collected at local time 09:00–11:00 am (Zou et al., 2015; Wu et al., 2019). This extensive sampling effort therefore generated detailed data of the monthly and yearly variations in the ponds.

2.3. Measurements of dissolved GHG concentrations

In order to measure dissolved CH_4 and N_2O concentrations, bubble-free water samples were collected from 20 cm below the water surface with a syringe (60-mL) equipped with a three-way stopcock (Wang et al., 2017; Borges et al., 2018;), each water sample was transferred into a glass serum bottle (55-mL). To stop the microbial activities, 0.2 mL $HgCl_2$ was added to water before closing the bottles (Borges et al., 2018; Zhang et al., 2013). The bottles were sealed with butyl rubber stoppers without headspace (Xiao et al., 2019; Webb et al., 2018) and transported in a cooler back to laboratory for analysis within 4–6 hr.

The headspace equilibration technique was used to analyze dissolved GHG concentrations (Davidson et al., 2015; Wang et al., 2021; Yu et al., 2017). Briefly, >99.999% purity nitrogen (N_2) gas was injected into every serum bottle to displace a 25-mL headspace. The bottles were than shaken vigorously for 10 minutes to create an equilibrium between the gaseous phase and the liquid phase. After settling for 30 min, 5 mL of the headspace gas was withdrawn for CH_4 measurement (Shimadzu GC-2010 with flame ionization detector, Kyoto, Japan) and 5 mL for N_2O measurement

(Shimadzu GC-2014 with electron capture detector, Kyoto, Japan). Calibration curves were produced with standard CH_4 gas (2, 8, 500 and 1000 ppm) and standard N_2O gas (0.3, 0.4 and 1.0 ppm). The original concentrations of dissolved CH_4 (or N_2O) were calculated from the headspace CH_4 (or N_2O) concentrations, taking into account the Bunsen gas solubility coefficients as a function of salinity and temperature (Farías et al., 2017; Brase et al., 2017; Weiss and Price, 1980).

2.4. Measurement of GHG emissions

The fluxes of CH_4 and N_2O across the water-air interface (WAI) were determined using the floating chamber method (Natchimuthu et al., 2016; Wu et al., 2021). The area and volume of the floating chamber are 0.1 m^2 and 5.2 L, respectively. The floating chamber was covered with reflective aluminum foil and fitted with styrofoam around the rim for floatation.

Gas flux measurements were conducted at the aforementioned three locations in each pond. At each location, a 60-mL gas sample was collected at an interval of 15-minute for 45 min with a syringe via a sampling port on the floating chamber. Gas samples were then injected into aluminum-foil gas sample bags (Dalian Delin Gas Packing Co., Ltd., China) and transported back to laboratory within 48 h for further analysis. In the laboratory, the GHG contents in the gas samples were determined by gas chromatographs (Shimadzu GC-2010 for CH_4 and Shimadzu GC-2014 for N_2O). CH_4 (mg m^{-2} h^{-1}) and N_2O (μg m^{-2} h^{-1}) fluxes across the WAI were calculated as the rate of change in the mass of CH_4 and N_2O per unit surface area per unit time (Yuan et al., 2021;

Yang et al., 2018). Total CH_4 and N_2O emissions over the farming period were calculated as the sum of the monthly values (Moore et al. 2011; Wu et al., 2018).

2.5. Estimation of diffusive and ebullitive CH_4 fluxes

CH_4 fluxes determined by the floating chamber include both diffusive and ebullitive fluxes (Chuang et al., 2017; Wu et al., 2019; Zhu et al., 2016). To partition the measurement between the two components, diffusive CH_4 flux (F_D, mg m^{-2} h^{-1}) across the water-atmosphere interface was estimated as follows (Musenze et al., 2014; Wanninkhof, 1992; White et al., 2021):

$$F_D = k_x \cdot (C_W - C_{eq})$$

where C_W (μmol L^{-1}) is the measured dissolved CH_4 concentration in the surface water; C_{eq} (μmol L^{-1}) is the equilibrium dissolved CH_4 concentration relative to the ambient atmospheric concentration at each sampling site; the gas transfer velocity k_x (m h^{-1}) was estimated from wind speed and temperature (Cole and Caraco, 1998). While different models exist to derive k_x (Klaus and Vachon, 2020), we used the model by Cole and Caraco (1998) because of the similar water surface areas and wind speeds in our study to the parameters used by them. Ebullitive CH_4 flux was estimated by subtracting the diffusive flux from the total CH_4 flux determined from the floating chamber (Xiao et al., 2017; Chuang et al., 2017; Yang et al., 2020b; Zhu et al., 2016).

2.6. Measurement of ancillary environmental parameters

In every sampling campaign, various environmental parameters were measured at 20 cm below water surface at each sampling location: pH and water temperature (T_W) by a portable meter (IQ150, IQ Scientific Instruments, U.S.A.); salinity by a salinity meter (Eutech Instruments-Salt6, USA), and dissolved oxygen (DO) by a multiparameter probe (550A YSI, USA). Meteorological variables (e.g., wind speed (W_S), air temperature (T_A), and air pressure (A_P)) were determined by a data logger (Vantage Pro 2, China) at the MRE. In addition, wind speed (1.5 m above the water surface) was determined at the ponds by a portable meter (Kestrel-3500, USA).

Water samples were collected at 20 cm below water surface at sampling locations using a 1.5-L organic glass hydrophore. All water samples were stored in an ice-packed cooler for later laboratory analysis within 4–6 hr. In the laboratory, water samples were filtered through cellulose acetate filters (0.45-µm Biotrans™ nylon membranes) and the filtrates were analyzed for the concentrations of dissolved organic carbon (DOC), PO_4^{3-}, NH_4^+-N, NO_3^--N, and total dissolved nitrogen (TDN). DOC was determined using a TOC Analyzer (TOC-$V_{CPH/CPN}$, Shimadzu, Kyoto, Japan) with a precision of ±1.0%. PO_4^{3-}, NH_4^+-N, NO_3^--N, and TDN were analyzed by a flow injection analyzer (Skalar Analytical SAN^{++}, The Netherlands) with a precision of ±3.0%, ±3.0%, ±3.0% and ±2.0%, respectively.

2.7. Calculation of CO_2-equivalent fluxes

We calculated the CO_2-equivalent emission based on IPCC methodology by multiplying CH_4 emission by a global warming potential value of 45 (based on a 100-year time horizon and a GWP value of 1 for CO_2) and N_2O emission by 270 (Neubauer and Megonigal, 2019). We also accounted for the GHG contribution of the aerator by multiplying its energy consumption by CO_2 emission factor for hydropower (10 g CO_2 per kWh; Hou et al., 2012).

2.8. Statistical analysis

Results were presented as mean ± 1SE. Statistical analyses were conducted in SPSS 22.0 (IBM, Armonk, NY, USA) with the significance level at 0.05. Two-way analysis of variance (two-way ANOVA) was used to examine the impacts of ponds, sampling time, and their interactions on GHG fluxes, dissolved GHG concentrations and surface water environmental properties. Pearson correlation analysis was applied to analyze the relationships between environmental properties and GHG fluxes or concentrations. Redundancy Analysis (RDA) was conducted to analyze the extent to which environmental parameters affected the spatiotemporal variations in GHG emissions, with T_W, pH, salinity, DO, DOC, PO_4^{3-}, NO_3^--N and NH_4^+-N, and TDN as the independent variables. RDA was done in CANOCO 5.0 (Microcomputer Power, Ithaca, USA). All graphics were generated with OriginPro version 7.5 (OriginLab Corporation, Northampton, MA, USA).

3. Results

3.1. Environmental parameters

The environmental conditions in the ponds over the study period were presented in Figure 2. There were no significant differences in mean T_W, pH, salinity and PO_4^{3-} among the ponds (p>0.05; Table S1), but there were significant variations for the other parameters. Overall, the mean DO (Figure 2d), NO_3^--N (Figure 2g), NH_4^+-N (Figure 2h) and TDN (Figure 2i) concentrations were significantly lower, while DOC concentrations (Figure 2e) were generally higher in non-aerated pond (NAP) than those in aerated ponds (APs) (p<0.05 or <0.01; Table S1).

3.2. Dissolved CH_4 and N_2O concentrations

Dissolved CH_4 concentration in the ponds was highly variable, ranging from 84.1 to 1980.4 nmol L^{-1} (Figure 3a), and it was always supersaturated with respect to the atmosphere. Across the two years, the mean CH_4 concentration was significantly higher in NAP (878.3 ± 132.5 nmol L^{-1}), followed by AP II (445.4 ± 94.4 nmol L^{-1}) and API (367.1 ± 61.3 nmol L^{-1}) (p<0.001; Table 1).

Dissolved N_2O concentration ranged from 2.1 to 26.2 nmol L^{-1} in the ponds (Figure 3b) and was always supersaturated with respect to the atmosphere. Over the two-year period, NAP had a significantly lower mean N_2O concentration (4.4 ± 0.6 nmol L^{-1}) than AP I (10.1 ± 1.8 nmol L^{-1}) and AP II (8.4 ± 1.3 nmol L^{-1}) ($p < 0.001$; Table 1).

3.3. CH_4 and N_2O emissions

The CH_4 fluxes ranged 0.23–36.49 mg m^{-2} h^{-1} in NAP, 0.06–22.89 mg m^{-2} h^{-1} in AP I, and 0.14–22.56 mg m^{-2} h^{-1} in AP II (Figure 4a). The respective mean flux was 7.56 ± 2.69 (NAP), 4.50 ± 1.73 (AP I) and 4.51 ± 1.82 mg m^{-2} h^{-1} (AP II). Despite no significant difference in average CH_4 fluxes between AP I and AP II ($p > 0.05$; Figure S1a), the average CH_4 flux in NAP was significantly higher than in the APs ($p < 0.05$; Table 2 and Figure S1a).

N_2O fluxes in NAP, AP I, and AP II ranged 2.39–20.77, 3.49–50.28, and 2.64–25.70

μg m^{-2} h^{-1} (Figure 4b), respectively. NAP had a significantly lower mean N_2O flux (6.98 ± 1.42 μg m^{-2} h^{-1}) than AP I (15.96 ± 3.48 μg m^{-2} h^{-1}) and AP II (11.72 ± 1.97 μg m^{-2} h^{-1}) during the study period ($p < 0.001$; Table 2, Figure S1b).

3.4. Diffusive and ebullitive fluxes of CH_4

The calculated mean CH_4 diffusive fluxes (see section 2.5) varied from 0.31 to 0.40 mg m^{-2} h^{-1} in NAP, 0.12 to 0.20 mg m^{-2} h^{-1} in AP I, and 0.13 to 0.20 mg m^{-2} h^{-1} in AP II. The respective CH_4 ebullitive fluxes were then estimated to be 4.96–9.47 (NAP), 3.45–5.23 (AP I) and 3.90–4.78 mg m^{-2} h^{-1} (AP II) (Figure 5). Overall, ebullition was estimated to account for the majority (94–96 %) of CH_4 emission. Over the farming period in the two consecutive years, NAP had a significantly higher mean CH_4 ebullitive flux (7.21 ± 2.71 mg m^{-2} h^{-1}) than AP I (4.34 ± 1.74 mg m^{-2} h^{-1}) and AP II (4.34 ± 1.83 mg m^{-2} h^{-1}) ($p < 0.001$).

3.5. CO_2-equivalent emissions of CH_4 and N_2O

Across all sampling campaigns, the aquaculture ponds were a net source of CH_4 and N_2O to the atmosphere. The combined CO_2-equivalent emissions were 22,780 (NAP), 12,806 (AP I) and 11,685 kg CO_2-eq ha^{-1} yr^{-1} (AP II) in 2019, and 12,473, 8,632 and 9,669 kg CO_2-eq ha^{-1} yr^{-1} in 2020, respectively (Figure 6). Energy consumption by the aerators added only 126–136 kg CO_2-eq ha^{-1} yr^{-1} in the aerated ponds.

Across the two consecutive years, the CO_2-equivalent emission from NAP averaged 17,626 kg CO_2-eq ha^{-1} yr^{-1}, which was 63% and 49% greater than that of AP I and AP II, respectively. CH_4 accounted for over 95% of the CO_2-equivalent emission in each pond

(Figure 6).

3.6. Relationships between gas fluxes and environmental parameters

Pearson correlation analyses indicated that CH_4 flux was correlated positively with T_W, DOC and NH_4^+-N ($p < 0.05$ or < 0.01; Table S2) and negatively with salinity, pH (Table S2) and DO (Figure S2a-S2c) ($p < 0.01$) (Table S2). N_2O flux was correlated positively with T_W, DO (Figure S2d-2f), NO_3^--N (Figure S3a-3c), NH_4^+-N (Figures S3d-3f) and TDN (Figures S3h-3i) ($p < 0.01$), and negatively with pH and DOC ($p < 0.05$ or < 0.01) (Table S2).

Based on RDA analysis, T_W, DO and TDN made significant contributions to the variations in CH_4 emission flux in both years. Combining all data, T_W had the largest explanatory power (47.5%), followed by DO (36.3%) and TDN (12.1%) (Figure 7). NO_3^--N and DO were the environmental parameters best explaining the variability in N_2O emission flux, with NO_3^--N accounting for the highest percentage (89.2% of all data) (Figure 7).

4. Discussion

4.1. Effects of aeration on water quality and shrimp yield

Shrimp aquaculture is generally maintained via daily supply of commercial aquatic feed, but only part of the feeds is converted into shrimp biomass (Avnimelech and Ritvo, 2003; Wang et al., 2018; Chen et al., 2016; Yang et al., 2020b), and the remainder is retained in the water column and sediment (Yang et al., 2021). In the present study, artificial aeration significantly increased the level of NH_4^+-N, NO_3^--N and TDN in the water column (Figures 2g-2i), similar to other studies in ponds (Zhu et al., 2020) and constructed wetlands (Ji et al., 2021; Maltais-Landry et al., 2009a, 2009b). This could be attributed to the increased DO level promoting remineralization of organic nitrogen from excess feeds and its subsequent release from the sediment (Han et al., 2018; Zhu et al., 2020).

Previous studies have suggested that intermittent artificial aeration can be a simple and effective management strategy to enhance water quality and increase animal yield in aquaculture systems (Boyd, 1998; Hu et al., 2013; Kosten et al., 2020; Zhu et al., 2020). Based on report by the farmer, the mean shrimp yield for the aerated ponds was 6,800 kg ha^{-1}, which was substantially higher than that for the non-aerated pond (5,200 kg ha^{-1}). The results suggested that continuous aeration could also increase shrimp yield.

4.2. Effects of aeration on CH_4 emission

Although some recent studies have shown that microbial CH_4 production can occur in oxic waters (Bogard et al., 2014; Günthel et al., 2019), conventional microbial methanogenesis in oxygen-deplete bottom water and sediment remains the principal source of CH_4 in shallow and eutrophic systems such as aquaculture ponds (Tong et al., 2021). Over the two years of our study, DO in APs was substantially higher than in NAP, showing a clear effect of aeration (Figure 2). Accordingly, the surface-water CH_4 concentration in NAP was much higher than in APs across all sampling campaigns (Figure 3). There were large month-to-month variations in CH_4 concentration, with lower values usually observed in the summer months, perhaps reflecting the increasing activity of CH_4 oxidizers. Surprisingly, CH_4 flux values were higher in the summer months (Figure 4), which were opposite to what would be expected from the lower surface-water CH_4 concentrations. A possible explanation is the higher sedimentary CH_4 production during the hot summer months, and the subsequent release via ebullition allowed CH_4 to by-pass oxidation in the water column (Rosentreter et al., 2017; Crawford et al., 2014; Wu et al., 2019; Xing et al., 2006). Indeed, ebullition was estimated to account for the overwhelming majority of CH_4 fluxes in all of the studied ponds (Figure 5), similar to other shallow and eutrophic inland waters (e.g., Wu et al., 2019; Zhang et al., 2020; Zhu et al., 2016; Yang et al., 2008). APs had comparable diffusive CH_4 flux to NAP, but considerably lower ebullitive flux, suggesting that the aerators were enough to lessen the anoxic condition in sediment.

In shrimp ponds, aeration could have opposing impacts on CH_4 emissions. On the one hand, increased oxygenation of the water could inhibit anaerobic microbial methanogenesis and promote CH_4 oxidation (Liu et al., 2016; Yuan et al., 2019). On the other hand, because CH_4 is only sparingly soluble in water, physical agitation by the aerators could increase diffusive exchange of CH_4 from water to air (Kosten et al., 2020; Yang et al., 2015). In our study, the inhibitive effects of aeration can be seen in the overall negative relationship between CH_4 fluxes and DO (Figure S2a-2c), similar to observations in aerated constructed wetlands (Ji et al., 2021; Maltais-Landry et al., 2009a; Liu et al., 2018). Yet, some data points from APs were noticeably above the trend line, indicating stronger CH_4 emissions than expected. Our observations suggest that aeration may increase CH_4 fluxes through physical agitation, especially in the mid-DO range (ca. 9-10 mg L^{-1}).

An earlier study estimated that whiteleg shrimp had an average feed conversion ratio of 1.33 in aerated ponds (Yang et al., 2021). From this we estimated the total amount of feeds applied to be ~9,044 kg ha^{-1} y^{-1}. Therefore, based on the reported shrimp yields, the excess feeds (i.e., feeds that were not converted to biomass) would average 26 mg m^{-2} h^{-1} in APs and 44 mg m^{-2} h^{-1} in NAP. In other words, we may expect 69% more carbon emission from unconsumed feeds in NAP compared to AP. Excess organic carbon would likely be converted to CO_2 in well-oxygenated water, but instead to CH_4 in oxygen-deplete water. Our measurements showed that CH_4 emission in NAP was 68% more than that in AP (7.56 vs. 4.50 mg m^{-2} h^{-1}). Hence, the low-oxygen condition in NAP essentially drove the conversion of all unconsumed feeds to CH_4 instead of CO_2. Considering that CH_4 is a much stronger GHG than CO_2, this shows the importance of aeration (or the lack of) in regulating the climate impact of the aquaculture ponds.

Taking together data across the two consecutive years, DO and T_w were the two key but opposing factors in determining the CH_4 emission flux (Figure 7). For the purpose of mitigating CH_4 emission from the shrimp ponds, while it would be difficult to manipulate T_W, DO can be easily increased with aerators. An interesting observation is the sizable positive effect TDN had on CH_4 emission; on the contrary, the presumptive substrate for methanogenesis, DOC, had weak effect on CH_4 emission (Figure 7). This perhaps indicates that the methanogen activity level was regulated by nitrogen availability.

4.3. Effects of aeration on N_2O emission

While methanogenesis is driven predominantly by anaerobic microbial processes in bottom water and sediment, N_2O can be produced via nitrification of NH_4^+-N and denitrification of NO_3^--N within the water column, with the two processes intertwined by a series of reduction-oxidation reactions (Beaulieu et al., 2015; Maavara et al., 2019; Yuan et al., 2021). Not surprisingly, the temporal change of N_2O emission flux (Figure 4b) mirrored that in dissolved N_2O concentration, and these two were positively correlated with both NO_3^--N and NH_4^+-N (Figure S3 and Table S2). Taking all data together, NO_3^--N explained most (89%) of the variability in N_2O flux (Figure 7), affirming the singular importance of nutrient loading in driving N_2O production in aquaculture ponds (Hu et al., 2013; Wu et al., 2018).

Unlike CH_4, N_2O is highly soluble in water. Therefore, its emission pathway is primarily through diffusive flux and not ebullition, and physical turbulence within the water column was expected to increase water-to-air N_2O flux (Hu et al., 2013; Kosten et al., 2020). Indeed, N_2O flux was consistently higher in APs than in NAP (Figure 4). There was an overall positive correlation between N_2O flux and DO across all measurements, with many of the data points from APs lying above the trend line (Figure S2d-2f), suggesting that physical agitation by the aerators enhanced N_2O gaseous exchange across the water-air interface.

4.4. Implications for global warming mitigation

With the wild stocks being depleted by overfishing, the world is increasingly turning towards aquaculture to satisfy its demand for aquatic animal proteins, particularly in developing countries (FAO, 2018; Hu et al., 2012; Yang et al., 2017). While small-hold aquaculture offers benefits including increasing food security, adding jobs and promoting rural economy (Béné et al., 2016; FAO, 2018; Hu et al., 2012), aquaculture boom can also raise environmental concerns including GHG emissions (MacLeod et al., 2020; Wu et al., 2018; Yuan et al., 2021). Although aquaculture ponds account for only ca. 1.8% and 0.3% of the global anthropogenic CH_4 and N_2O emissions, respectively (Yuan et al., 2019), their climate impacts can be significant in regions where small aquaculture ponds are widespread (FAO, 2018), such as along China's coast (Duan et al., 2020; Ren et al., 2019). As shown in this study, the small shrimp ponds in MRE in southeastern China were strong CH_4 and N_2O emitters.

Improvement of management practices will be key to reducing GHG emissions from aquaculture ponds and achieving a clean and sustainable production. Aeration is a common practice in aquaculture, but it may have opposite effects on GHG fluxes from the ponds. Our results showed that aeration increased N_2O emission by 98%, but decreased CH_4 emission by 40%. In order to place the gas flux values in the context of climate impact, we calculated the CO_2-equivalent emission based on the IPCC model for SGWP (IPCC, 2013; Neubauer and Megonigal, 2019). Our calculations showed that the average combined emission in non-aerated ponds (342 mg CO_2-eq m^{-2} h^{-1}) was substantially larger than the global average for reservoirs (242 mg CO_2-eq m^{-2} h^{-1}) (Deemer et al., 2016) and the average value for China's lakes and reservoirs (Li et al., 2018), whereas the combined emission in aerated ponds (206 mg CO_2-eq m^{-2} h^{-1}) was considerably lower. CO_2 emission due to electricity consumption by the aerators was negligible. Overall, CH_4 emission was vastly more important than N_2O emission in terms of centennial-scale climate impact of the shrimp ponds, and aeration was able to decrease the annual CO_2-equivalent emission of the shrimp ponds by 40% (Figure 6).

4.5. Recommendations for future research

Our data showed that water temperature had a positive influence on CH_4 emission. The subtropical location of our study site and the exposed nature of the ponds inevitably led to high water temperatures. Future study may consider testing the effect of shading as a way to lower the water temperature and CH_4 emission. Because N_2O emission was mostly influenced by NO_3^--N, a better management of nutrient loading into the ponds may help to reduce N_2O emission.

Instead of paddlewheel aerators, some farmers use air diffusers for aeration, which sit at the bottom of the ponds and release air bubbles. While diffusers may oxygenate the entire water column more effectively than paddlewheels, rising air bubbles may strip the water column of dissolved GHGs and greatly increase water-to-air GHG fluxes (Hu et al., 2012; Yang et al., 2020b). A comparative study of the different aerator designs will be useful to produce appropriate recommendations to farmers for mitigating GHG emissions.

Artificial aeration can lead to high DO level in water column, which would enhance CH_4 oxidation to CO_2 (Casper et al., 2000; Kosten et al., 2020) and add to CO_2 emission to air. Because CO_2 emissions were not measured in the present study, the total CO_2-equivalent emission from the aerated ponds could have been underestimated. Further study on the effects of aeration on CO_2 emissions from aquaculture ponds is needed.

While the physical effects of aeration on GHG emissions are not expected to depend on the species, aquaculture ponds with other species (shell- or fin-fish) will likely develop different microbial communities and therefore the magnitude of GHG emissions may be different. Expanding the study to other aquaculture systems and species will help generate a more detailed understanding of the comprehensive climate impact of the aquaculture sector.

5. Conclusions

This study quantified the effects of artificial aeration on GHG emissions from aquaculture ponds. Our results indicate that artificial aeration had opposite effects on N_2O and CH_4 emissions: It increased N_2O emission likely via physical agitation of the water column, but decreased CH_4 emission likely by suppressing anaerobic methanogenesis and promoting CH_4 oxidation. The combined annual CO_2-equivalent emission from CH_4 and N_2O in non-aerated pond was >1.6 times higher than that in aerated ponds, with CH_4 being the main contributor. These findings suggest that increasing the DO level by artificial aeration is a simple, inexpensive and effective management strategy to mitigate GHG emissions from aquaculture ponds.

Acknowledgements

This research was funded by the National Natural Science Foundation of China (NNSFC) (No. 41801070, 41671088), the National Natural Science Foundation of Fujian Province (NNSFF) (No. 2018J01737, 2020J01136), and the Minjiang Scholar Programme.

References

Adegbeye, M.J., Elghandour, M.M.M.Y., Monroy, J.C., Abegunde, T.O., Salem, A.Z.M., Barbabosa-Pliego, A., Faniyi, T.O., 2019. Potential influence of Yucca extract as feed additive on greenhouse gases emission for a cleaner livestock and aquaculture farming-A review. J. Clean. Prod. 239, 118074. https://doi.org/10.1016/j.jclepro.2019.118074

Avnimelech, Y., Ritvo, G., 2003. Shrimp and fish pond soils: processes and management. Aquaculture 220, 549–567. https://doi.org/10.1016/S0044-8486(02)00641-5

Beaulieu, J.J., Nietch, C.T., Young, J.L., 2015. Controls on nitrous oxide production and consumption in reservoirs of the Ohio River Basin. J. Geophys. Res. Biogeosci. 120 (10), 1995–2010. https://doi.org/10.1002/2015JG002941

Béné, C., Arthur, R., Norbury, H., Allison, E.H., Beveridge, M., Bush, S., Campling, L., Leschen, W., Little, D., Squires, D., Thilsted, S.H., Troell, M., Williams, M., 2016. Contribution of fisheries and aquaculture to food security and poverty reduction: assessing the current evidence. World Dev. 79, 177–196.

Bogard, M.J., del Giorgio, P.A., Boutet, L., Chaves, M.C.G., Prairie1, Y.T., Merante, A., Derry, A.M., 2014. Oxic water column methanogenesis as a major component of aquatic CH_4 fluxes. Nat. Commun. 5, 5350. http://dx.doi.org/10.1038/ncomms6350

Borges, A.V., Darchambeau, F., Lambert, T., Bouillon, S., Morana, C., Brouyère, S., Hakoun, V., Jurado, A., Tseng, H.-C., Descy, J.-P., Roland, F.A.E., 2018. Effects of agricultural land use on fluvial carbon dioxide, methane and nitrous oxide concentrations in a large European river, the Meuse (Belgium). Sci. Total Environ. 610-611, 342–355. http://dx.doi.org/10.1016/j.scitotenv.2017.08.047

Boyd, C.E., 1998. Pond water aeration systems. Aquac. Eng. 18, 9–40. https://doi.org/10.1016/S0144-8609(98)00019-3

Brase, L., Bange, H.W., Lendt, R., Sanders, T., Dähnke, K., 2017. High resolution measurements of nitrous oxide (N_2O) in the Elbe Estuary. Front. Mar. Sci. 4, 162. https://doi.org/10.3389/fmars.2017.00162

Bureau of Fisheries of the Ministry of Agriculture (BFMA), 2019. China Fishery Statistics Yearbook. China Agriculture Press, Beijing (in Chinese).

Casper, P., Maberly, S.C., Hall, G.H., Finlay, B.J., 2000. Fluxes of methane and carbon dioxide from a small productive lake to the atmosphere. Biogeochemistry 49, 1–19.

Chen, Y., Dong, S.L., Wang, F., Gao, Q.F., Tian, X.L., 2016. Carbon dioxide and methane fluxes from feeding and no-feeding mariculture ponds. Environ. Pollut. 212, 489–497. http://dx.doi.org/10.1016/j.envpol.2016.02.039

Crawford, J.T., Stanley, E.H., Spawn, S.A., Finlay, J.C., Loken, L.C., Striegl, R.G., 2014. Ebullitive methane emissions from oxygenated wetland streams. Glob. Change Biol. 20 (11), 3408–3422. https://doi.org/10.1111/gcb.12614

Chuang, P.-C., Young, M.B., Dale, A.W., Miller, L.G., Herrera-Silveira, J.A., Paytan, A., 2017. Methane fluxes from tropical coastal lagoons surrounded by mangroves, Yucatán, Mexico. J. Geophys. Res. Biogeosci. 122 (5), 1156–1174. http://dx.doi.org/10.1002/2017JG003761

Cole, J.J., Caraco, N.F., 1998. Atmospheric exchange of carbon dioxide in a low-wind oligotrophic lake measured by the addition of SF_6. Limnol. Oceanogr. 43(4), 647-656. https://doi.org/10.4319/lo.1998.43.4.0647

Davidson, T.A., Audet, J., Svenning, J.-C., Lauridsen, T.L., Søndergaard, M., Landkildehus, F., Larsen, S.E., Jeppesen, E., 2015. Eutrophication effects on greenhouse gas fluxes from shallow-lake mesocosms override those of climate warming. Global Change Biol. 21, 4449−4463. https://doi.org/10.1111/gcb.13062

Deemer, B.R., Harrison, J.A., Li, S.Y., Beaulieu, J.J., Delsontro, T., Barros, N., Bezerra-Neto, J.F., Powers, S.M., Santos, M.A.D., Vonk, J.A., 2016. Greenhouse gas emissions from reservoir water surfaces: a new global synthesis. BioScience 66, 949–964. https://doi.org/10.1093/biosci/biw117

Duan, Y.Q., Li, X., Zhang, L.P., Chen, D., Liu, S.A., Ji, H.Y., 2020. Mapping national-scale aquaculture ponds based on the Google Earth Engine in the Chinese coastal zone. Aquaculture 520, 734666. https://doi.org/10.1016/j.aquaculture.2019.734666

FAO, 2018. The State of World Fisheries and Aquaculture 2018-Meeting the Sustainable Development Goals. FAO, Rome.

Farías, L., Sanzana, K., Sanhueza-Guevara, S., Yevenes, M.A., 2017. Dissolved methane distribution in the Reloncaví Fjord and adjacent marine system during austral winter (41°-43° S). Estuar. Coast. 40(6), 1592–1606. https://doi.org/10.1007/s12237-017-0241-2

Grinham, A., Albert, S., Deering, N., Dunbabin, M., Bastviken, D., Sherman, B., Lovelock, C.E., Evans, C.D., 2018. The importance of small artificial water bodies as sources of methane emissions in Queensland, Australia. Hydrol. Earth Syst. Sci. 22, 5281–5298. https://doi.org/10.5194/hess-22-5281-2018

Günthel, M., Donis, D., Kirillin, G., Ionescu, D., Bizic, M., McGinnis, D.F., Grossart, H.-P., Tang, K.W., 2019. Contribution of oxic methane production to surface methane emission in lakes and its global importance. Nat. Commun. 10, 5497. https://doi.org/10.1038/s41467-019-13320-0

Han, Z.L., Sun, D.Z., Wang, H., Li, R.Y., Bao, Z.Y., Qi, F., 2018. Effects of ambient temperature and aeration frequency on emissions of ammonia and greenhouse gases from a sewage sludge aerobic composting plant. Bioresource Technol. 270, 457–466. https://doi.org/10.1016/j.biortech.2018.09.048

Hou, P., Wang, H.T., Zhang, H., Fan, C.D., Huang, N., 2012. Greenhouse gas emission factors of Chinese power grids for organization and product carbon footprint. China

Environ. Sci. 32(6): 961–967.

Hu, Z., Lee, J.W., Chandran, K., Kim, S., Sharma, K., Khanal, S.K., 2012. Nitrous oxide (N_2O) emission from aquaculture: a review. Environ. Sci. Technol. 46, 6470–6480. https://doi.org/10.1021/es300110x

Hu, Z., Lee, J.W., Chandran, K., Kim, S., Sharma, K., Brotto, A.C., Khanal, S.K., 2013. Nitrogen transformations in intensive aquaculture system and its implication to climate change through nitrous oxide emission. Bioresour. Technol. 130, 314–320. http://dx.doi.org/10.1016/j.biortech.2012.12.033

IPCC, 2013. Climate Change 2013: The Physical Science Basis. In: Stocker, T.F. (Ed.), Contribution of Working Group I to the Fifth Assessment Report of the Intergovernmental Panel on Climate Change. Cambridge Univ. Press and others [eds.] https://doi.org/10.1017/CBO9781107415324

IPCC, 2019. In: Calvo Buendia, E., Tanabe, K., Kranjc, A., Baasansuren, J., Fukuda, M., Ngarize, S. (Eds.), 2019 Refinement to the 2006 IPCC Guidelines for National Greenhouse Gas Inventories, Volum 4. IPCC, Switzerland. Kanagawa, Japan Chapter 07.

Ji, B.H., Chen, J.Q., Mei, J., Chang, J.J., Li, X., Jia, W., Qu, Y., 2020. Roles of biochar media and oxygen supply strategies in treatment performance, greenhouse gas emissions, and bacterial community features of subsurface-flow constructed wetlands. Bioresource Technol. 302, 122890. https://doi.org/10.1016/j.biortech.2020.122890

Ji, B. H., Chen, J.Q., Li, W., Mei, J., Yang, Y., Chang, J.J., 2021. Greenhouse gas emissions from constructed wetlands are mitigated by biochar substrates and distinctly affected by tidal flow and intermittent aeration modes. Environ. Pollut. 271, 116328. https://doi.org/10.1016/j.envpol.2020.116328

Klaus, M., Vachon, D. 2020. Challenges of predicting gas transfer velocity from wind measurements over global lakes. Aquat. Sci. 82, 53. https://doi.org/10.1007/s00027-020-00729-9

Kosten, S., Almeida, R.M., Barbosa, I., Mendonç, R., Muzitano, I.S., Oliveira-Junior, E.S., Vroom, R.J.E., Wang, H.J., Barros, N., 2020. Better assessments of greenhouse gas emissions from global fish ponds needed to adequately evaluate aquaculture footprint. Sci. Total Environ, 748, 141247. https://doi.org/10.1016/j.scitotenv.2020.141247

Li, S.Y., Bush, R.T., Santos, I.R., Zhang, Q.F., Song, K.S., Mao, R., Wen, Z.D., Lu, X.X., 2018. Large greenhouse gases emissions from China's lakes and reservoirs. Water Res. 147, 13–24. https://doi.org/10.1016/j.watres.2018.09.053

Liu, S.W., Hu, Z.Q., Wu, S., Li, S.Q., Li, Z.F., Zou, J.W., 2016. Methane and nitrous oxide emissions reduced following conversion of rice paddies to inland crabfish aquaculture in southeast China. Environ. Sci. Technol. 50 (2), 633–642. https://doi.org/10.1021/acs.est.5b04343

Liu, X.L., Zhang, K., Fan, L.Q., Luo, H.B., Jiang, M.S., Anderson, B.C., Li, M., Huang, B., Yu, L.J., He, G.Z., Wang, J.T., Pu, A.P., 2018. Intermittent micro-aeration control of methane emissions from an integrated vertical-flow constructed wetland during agricultural domestic wastewater treatment. Environ. Sci. Pollut. R. 25, 24426–24444. https://doi.org/10.1007/s11356-018-2226-5

Maavara, T., Lauerwald, R., Laruelle, G.G., Akbarzadeh, Z., Bouskill, N.J., Van Cappellen, P., Regnier, P., 2019. Nitrous oxide emissions from inland waters: Are IPCC estimates too high? Global Change Biology, 25(2), 473–488. https://doi.org/10.1111/gcb.14504

MacLeod, M.J.; Hasan, M.R.; Robb, D.H.; Mamun-Ur-Rashid, M., 2020. Quantifying greenhouse gas emissions from global aquaculture. Sci. Rep. 10(1), 1–8. https://doi.org/10.1038/s41598-020-68231-8

Maltais-Landry, G., Maranger, R., Brisson, J., Chazarenc, F., 2009a. Greenhouse gas production and efficiency of planted and artificially aerated constructed wetlands. Environ. Pollut. 157, 748–754. https://doi.org/10.1016/j.envpol.2008.11.019

Maltais-Landry, G., Maranger, R., Brisson, J., 2009b. Effect of artificial aeration and macrophyte species on nitrogen cycling and gas flux in constructed wetlands. Ecol.

Eng. 35, 221–229. https://doi.org/10.1016/j.ecoleng.2008.03.003

Moore, T.R., De Young, A., Bubier, J.L., Humphreys, E.R., Lafleur, P.M., Roulet, N.T., 2011. A multi-year record of methane flux at the Mer Bleue Bog, southern Canada. Ecosystems 14, 646-657. https://doi.org/10.1007/s10021-011-9435-9

Musenze, R.S., Grinham, A., Werner, U., Gale, D., Sturm, K., Udy, J., Yuan, Z.G., 2014. Assessing the spatial and temporal variability of diffusive methane and nitrous oxide emissions from subtropical freshwater reservoirs. Environ. Sci. Technol. 48, 14499–14507. https://doi.org/10.1021/es505324h

Natchimuthu, S., Sundgren, I., Gålfalk, M., Klemedtsson, L., Crill, P., Danielsson, Å., Bastviken, D., 2016. Spatio-temporal variability of lake CH_4 fluxes and its influence on annual whole lake emission estimates. Limnol. Oceanogr. 61 (S1), S13–S26. https://doi.org/10.1002/lno.10222

National Oceanic and Atmospheric, 2021a. Carbon cycle greenhouse gases: Trends in Atmospheric Methane. Available in: https://gml.noaa.gov/ccgg/trends_ch4/

National Oceanic and Atmospheric, 2021b. Carbon cycle greenhouse gases: Trends in Atmospheric Nitrous Oxide. Available in: https://gml.noaa.gov/ccgg/trends_n2o/

Neubauer, S.C., Megonigal, J.P., 2019. Correction to: Moving beyond global warming potentials to quantify the climatic role of ecosystems. Ecosystems 22, 1931–1932. https://doi.org/10.1007/s10021-019-00422-5

Ren, C.Y., Wang, Z.M., Zhang, Y.Z., Zhang, B., Chen, L., Xia, Y.B., Xiao, X.M., Doughty, R.B., Liu, M.Y., Jia, M., Mao, D.H., Song, K.S., 2019. Rapid expansion of coastal aquaculture ponds in China from Landsat observations during 1984–2016. Int. J. Appl. Earth Obs. 82, 101902. https://doi.org/10.1016/j.jag.2019.101902

Rosentreter, J.A., Maher, D.T., Ho, D.T., Call, M., Barr, J.G., Eyre, B.D., 2017. Spatial and temporal variability of CO_2 and CH_4 gas transfer velocities and quantification of the CH_4 microbubble flux in mangrove dominated estuaries. Limnol. Oceanogr. 62(2), 561–578. https://doi.org/10.1002/lno.10444

Soares, D.C.E. Henry-Silva, G.G., 2019. Emission and absorption of greenhouse gases generated from marine shrimp production (*Litopeneaus vannamei*) in high salinity. J. Clean. Prod. 218, 367-376. https://doi.org/10.1016/j.jclepro.2019.02.002

Tong, C., Bastviken, D., Tang, K.W., Yang, P., Yang, H., Zhang, Y.F., Guo, Q.Q., Lai, D.Y.F., 2021. Annual CO_2 and CH_4 fluxes in coastal earthen ponds with *Litopenaeus vannamei* in southeastern China. Aquaculture 545, 737229. https://doi.org/10.1016/j.aquaculture.2021.737229

Tong, C., Morris, J.T., Huang, J.F., Xu, H., Wan, S.A., 2018. Changes in pore-water chemistry and methane emission following the invasion of *Spartina alterniflora* into an oliogohaline marsh. Limnol. Oceanogr. 63(1), 384–396. https://doi.org/10.1002/lno.10637

Tong, C., Wang, W.Q., Huang, J.F., Gauci, V., Zhang, L.H., Zeng, C.S., 2012. Invasive alien plants increase CH_4 emissions from a subtropical tidal estuarine wetland. Biogeochemistry 111, 677–693. https://doi.org/10.1007/s10533-012-9712-5

Xiao, Q.T., Hu, Z.H., Fu, C.S., Bian, H., Lee, X.H., Chen, S.T., Shang, D.Y., 2019. Surface nitrous oxide concentrations and fluxes from water bodies of the agricultural watershed in Eastern China. Environ. Pollut. 251, 185–192. https://doi.org/10.1016/j.envpol.2019.04.076

Xiao, Q.T., Zhang, M., Hu, Z.H., Gao, Y.Q., Hu, C., Liu, C., Liu, S.D., Zhang, Z., Zhao, J.Y., Xiao, W., Lee, X., 2017. Spatial variations of methane emission in a large shallow eutrophic lake in subtropical climate. J. Geophys. Res.- Biogeo. 122(7), 1597-1614. https://doi.org/10.1002/2017jg003805

Wang, J. W., Wu, W., Zhou, X.D., Huang, Y.Q., Guo, M.J., 2021. Nitrous oxide (N_2O) emissions from the high dam reservoir in longitudinal range-gorge regions on the Lancang-Mekong River, southwest China. J. Environ. Manage. 295, 113027. https://doi.org/10.1016/j.jenvman.2021.113027

Wang, Q., Liu, H., Sui, J., 2018. Mariculture: developments, present status and prospects. In: Gui, J.F., Tang, Q., Li, Z., Liu, J., De Silva, S.S. (Eds.), Aquaculture in China: Success Stories and Modern Trends. John Wiley & Sons Ltd, Hoboken, N.J, pp. 38–

54.

Wanninkhof, R., 1992. Relationship between wind speed and gas exchange over the ocean. J. Geophys. Res. Oceans 97(C5), 7373-7382. https://doi.org/10.1029/92JC00188

Webb, J.R., Santos, I.R., Maher, D.T., Macdonald, B., Robson, B., Isaac, P., McHugh, I., 2018. Terrestrial versus aquatic carbon fluxes in a subtropical agricultural floodplain over an annual cycle. Agr. Forest Meteorol. 260–261, 262–272. https://doi.org/10.1016/j.agrformet.2018.06.015

Weiss, R.F., Price, B.A., 1980. Nitrous oxide solubility in water and seawater. Mar. Chem. 8(4), 347–359. https://doi.org/10.1016/0304-4203(80)90024-9

White, S.A., Santos, I.R., Conrad, S.R., Sanders, C.J., Hessey, S., 2021. Large aquatic nitrous oxide emissions downstream of intensive horticulture driven by rain events. J. Hydrol. 596, 126066. https://doi.org/10.1016/j.jhydrol.2021.126066

Williams, J., Crutzen, P. J., 2010. Nitrous oxide from aquaculture. Nat. Geosci. 3(3), 143–143.

Wu, S., Hu, Z. Q., Hu, T., Chen, J., Yu, K., Zou, J. W., Liu, S. W., 2018. Annual methane and nitrous oxide emissions from rice paddies and inland fish aquaculture wetlands in southeast China. Atmos. Environ. 175, 135-144. https://doi.org/10.1016/j.atmosenv.2017.12.008

Wu, S., Li, S.Q., Zou, Z.H., Hu, T., Hu, Z.Q., Liu, S.W., Zou, J.W., 2019. High methane emissions largely attributed to ebullitive fluxes from a subtropical river draining a rice paddy watershed in China. Environ. Sci. Technol. 53, 349–3507. https://doi.org/10.1021/acs.est.8b05286

Wu, S., Zhang, T.R., Fang, X.T., Hu, Z.Q., Hu, J., Liu, S.W., Zou, J.W., 2021. Spatial-temporal variability of indirect nitrous oxide emissions and emission factors from a subtropical river draining a rice paddy watershed in China Agr. Forest Meteorol. 307, 108519. https://doi.org/10.1016/j.agrformet.2021.108519

Xing, Y.P., Xie, P., Yang, H., Wu, A.P., Ni, L.Y., 2006. The change of gaseous carbon fluxes following the switch of dominant producers from macrophytes to algae in a shallow subtropical lake of China. Atmos. Environ. 40, 8034-8043. https://doi.org/10.1016/j.atmosenv.2006.05.033

Yang, H., Andersen, T., Dörsch, P., Tominaga, K., T hrane, J.E., Hessen, D.O., 2015. Greenhouse gas metabolism in Nordic boreal lakes. Biogeochemistry 126, 211-225. https://doi.org/10.1007/s10533-015-0154-8

Yang, H., Ma, M., Thompson, J.R., Flower, R.J., 2017. Reform China's fisheries subsidies. Science 356(6345), 1343-1343. https://doi.org/10.1126/science.aan8389

Yang, H., Xing, Y., Xie, P., Ni, L., Rong, K., 2008. Carbon source/sink function of a subtropical, eutrophic lake determined from an overall mass balance and a gas exchange and carbon burial balance. Environ. Pollut. 151, 559-568. https://doi.org/10.1016/j.envpol.2007.04.006

Yang, P., Lai, D.Y.F., Jin, B.S., Bastviken, D., Tan, L.S., Tong, C., 2017. Dynamics of dissolved nutrients in the aquaculture shrimp ponds of the Min River estuary, China: Concentrations, fluxes and environmental loads. Sci. Total Environ. 603–604, 256–267. http://dx.doi.org/10.1016/j.scitotenv.2017.06.074

Yang, P., Yang,, H., Lai, D.Y.F., Guo, Q.Q., Zhang, Y.F., Tong, C., Xu, C.B., Li, X.F., 2020a. Large contribution of non-aquaculture period fluxes to the annual N_2O emissions from aquaculture ponds in Southeast China. J. Hydrol. 582, 124550. https://doi.org/10.1016/j.jhydrol.2020.124550

Yang, P., Zhang, Y.F., Yang, H., Guo, Q.Q., Lai, D.Y.F., Zhao, G.H., Li, L., Tong, C., 2020b. Ebullition was a major pathway of methane emissions from the aquaculture ponds in southeast China. Water Res. 184, 116176. https://doi.org/10.1016/j.watres.2020.116176

Yang, P., Zhang, Y.F., Lai, D.Y.F., Tan, L.S., Jin, B.S., Tong, C., 2018. Fluxes of carbon dioxide and methane across the water–atmosphere interface of aquaculture shrimp ponds in two subtropical estuaries: The effect of temperature, substrate, salinity and nitrate. Sci. Total Environ. 635, 1025–1035.

https://doi.org/10.1016/j.scitotenv.2018.04.102
Yang, P., Zhao, G.H., Tong, C., Tang, K.W., Lai, D.Y.F., Li, L., Tang, C., 2021. Assessing nutrient budgets and environmental impacts of coastal land-based aquaculture system in southeastern China. Agr. Ecosyst. Environ. 322, 107662. https://doi.org/10.1016/j.agee.2021.107662
Yu, Z.J., Deng, H.G., Wang, D.Q., Ye, M.W., Tan, Y.J., Li, Y.J., Chen, Z.L., Xu, S.Y., 2013. Nitrous oxide emissions in the shanghai river network: Implications for the effects of urban sewage and IPCC methodology. Global Change Biol. 19(10), 2999–3010. https://doi.org/10.1111/gcb.12290
Yuan, J.J., Xiang, J., Liu, D.Y., Kang, H., He, T.H., Kim, S., Lin, Y.X., Freeman, C., Ding, W.X., 2019. Rapid growth in greenhouse gas emissions from the adoption of industrial-scale aquaculture. Nat. Clim. Change 9 (4), 318–322. https://doi.org/10.1038/s41558-019-0425-9
Yuan, J.J., Liu, D.Y., Xiang, J., He, T.H., Kang, H., Ding, W.X., 2021. Methane and nitrous oxide have separated production zones and distinct emission pathways in freshwater aquaculture ponds. Water Res. 190, 116739. https://doi.org/10.1016/j.watres.2020.116739
Yu, Z.J., Wang, D.Q., Li, Y.J., Deng, H.G., Hu, B.B., Ye, M.W., Zhou, X.H., Da, L.J., Chen, Z.L., Xu, S.Y., 2017. Carbon dioxide and methane dynamics in a human-dominated lowland coastal river network (Shanghai, China). J. Geophys. Res. Biogeosci. 122 (7), 1738–1758. https://doi.org/10.1002/2017JG003798
Zhao, J.Y., Zhang, M., Xiao, W., Jia, L., Zhang, X.F., Wang, J., Zhang, Z., Xie, Y.H., Pu, Y.N., Liu, S.D., Feng, Z.Z., Lee, X.H., 2021. Large methane emission from freshwater aquaculture ponds revealed by long-term eddy covariance observation. Agr. Forest Meteorol. 308-309, 108600. https://doi.org/10.1016/j.agrformet.2021.108600
Zhang, L., Wang, L., Yin, K.D., Lü, Y., Zhang, D.R., Yang, Y.Q., Huang, X.P., 2013. Pore water nutrient characteristics and the fluxes across the sediment in the Pearl River

estuary and adjacent waters, China. Estuar. Coast. Shelf Sci. 133, 182–192. https://doi.org/10.1016/j.ecss.2013.08.028

Zhang, L.W., Xia, X.H., Liu, S.D., Zhang, S.B., Li, S.L., Wang, J.F., Wang, G.Q., Gao, H., Zhang, Z.R., Wang, Q.R., Wen, W., Liu, R., Yang, Z.F., Stanley, E.H., Raymond, P.A., 2020. Significant methane ebullition from alpine permafrost rivers on the East Qinghai–Tibet Plateau. Nat. Geosci. 13, 349–354. https://doi.org/10.1038/s41561-020-0571-8

Zou, X.X., Li, Y.E, Li, K., Cremades, R., Gao, Q.Z., Wan, Y.F., Qin, X.B., 2015. Greenhouse gas emissions from agricultural irrigation in China. Mitig. Adapt. Strateg. Glob. Change 20 (2), 295–315. https://doi.org/10.1007/s11027-013-9492-9

Zhu, D., Wu, Y., Chen, H., He, Y. X., Wu, N., 2016. Intense methane ebullition from open water area of a shallow peatland lake on the eastern Tibetan Plateau. Sci. Total Environ. 542, 57–64. https://doi.org/10.1016/j.scitotenv.2015.10.087

Zhu, D.T., Cheng, X.J., Sample, D.J., Yazdi, M.N., 2020. Effect of intermittent aeration mode on nitrogen concentration in the water column and sediment pore water of aquaculture ponds. J. Environ. Sci. 90, 331–342. https://doi.org/10.1016/j.jes.2019.11.022

Table 1 Results of two-way ANOVAs (with sampling date specified as the random term) on the effect of sampling ponds, sampling years and their interactions on the dissolved CH_4 and N_2O concentrations in the aquaculture ponds.

	df	**Dissolved CH_4 concentration**				**Dissolved N_2O concentration**			
		Sum of squares	*Mean square*	*F values*	*P values*	*Sum of squares*	*Mean square*	*F values*	*P values*
Sampling ponds	2	6.367	3.183	21.014	<0.001	728.558	364.279	16.566	<0.001
Sampling years	1	0.005	0.005	0.034	=0.854	552.807	552.807	25.139	<0.001
Sampling ponds × years	2	0.117	0.059	0.387	=0.680	48.392	24.196	1.100	=0.336
Residuals		18.178	0.151			2638.802	21.990		

Table 2 Results of two-way ANOVAs (with sampling date specified as the random term) on the effect of sampling ponds, sampling years and their interactions on CH_4 and N_2O fluxes from the aquaculture ponds.

	df	**CH_4 fluxes**				**N_2O fluxes**			
		Sum of squares	*Mean square*	*F values*	*P values*	*Sum of squares*	*Mean square*	*F values*	*P values*
Sampling ponds	2	261.710	130.855	2.135	=0.040	1694.630	847.315	10.431	<0.001
Sampling years	1	167.716	167.716	2.737	=0.101	2279.309	2279.309	28.059	<0.001
Sampling ponds × years	2	74.263	37.131	0.606	=0.547	311.738	155.869	28.059	=0.151
Residuals		7353.174	61.276			9747.972	81.233		

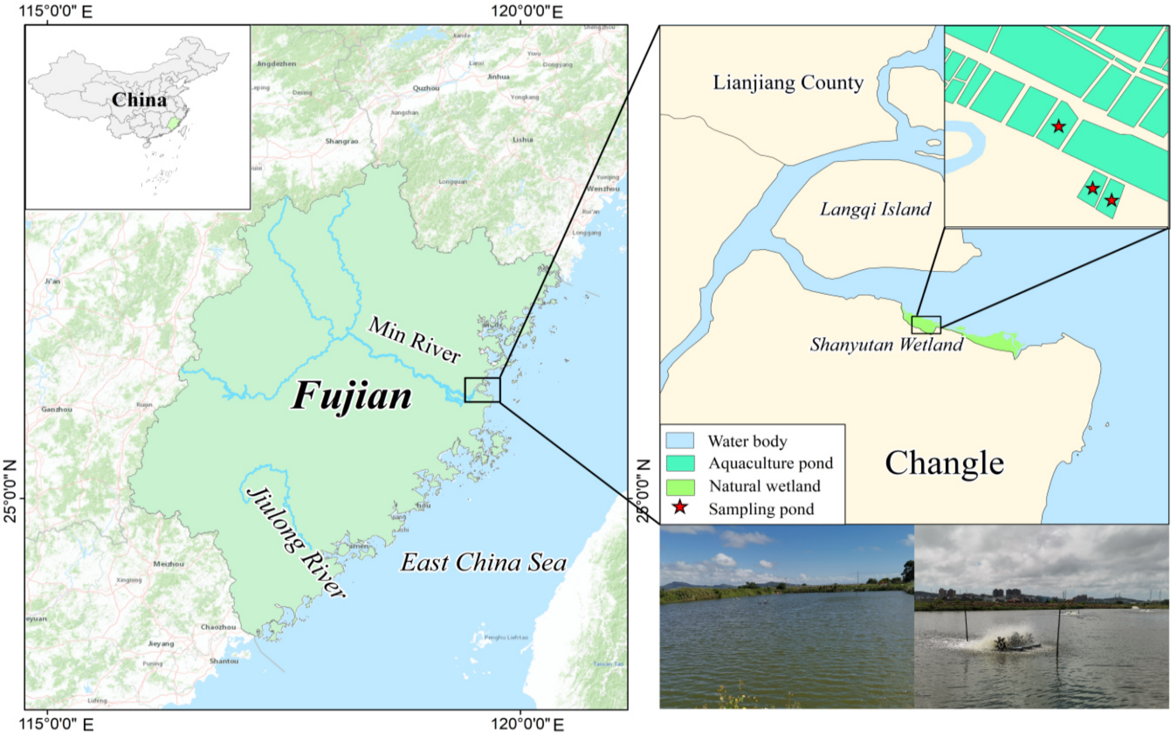

Figure 1. Location of the study area and aquaculture ponds in the Min River Estuary, Southeast China.

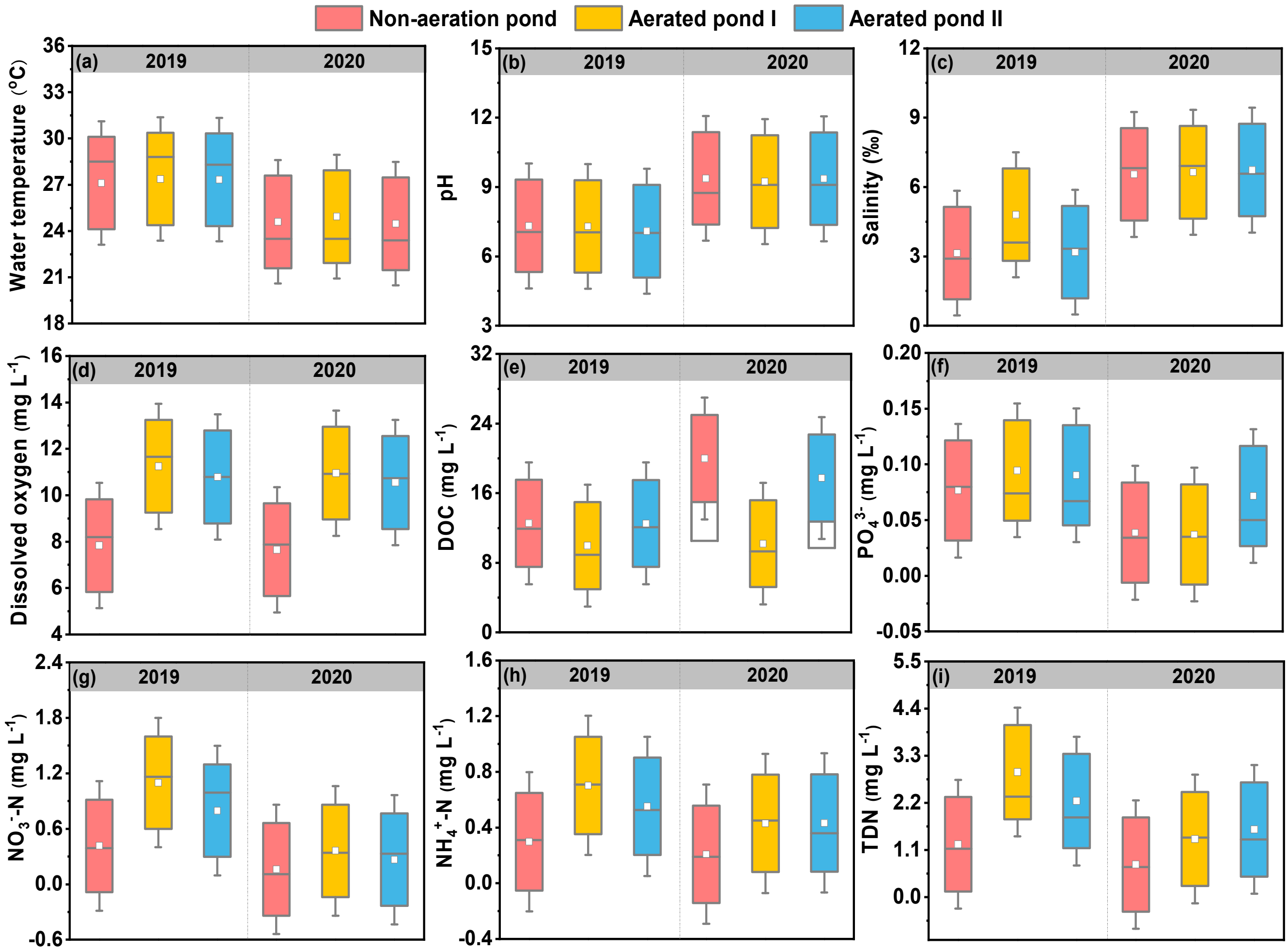

Figure 2. Boxplots of environmental parameters in the aquaculture ponds during the farming period in 2019 and 2020. Each box shows the quartiles and median, while the square and whiskers represent the mean and values within 1.5 times of the interquartile range, respectively. DOC represents dissolved organic carbon and TDN represents total dissolved nitrogen.

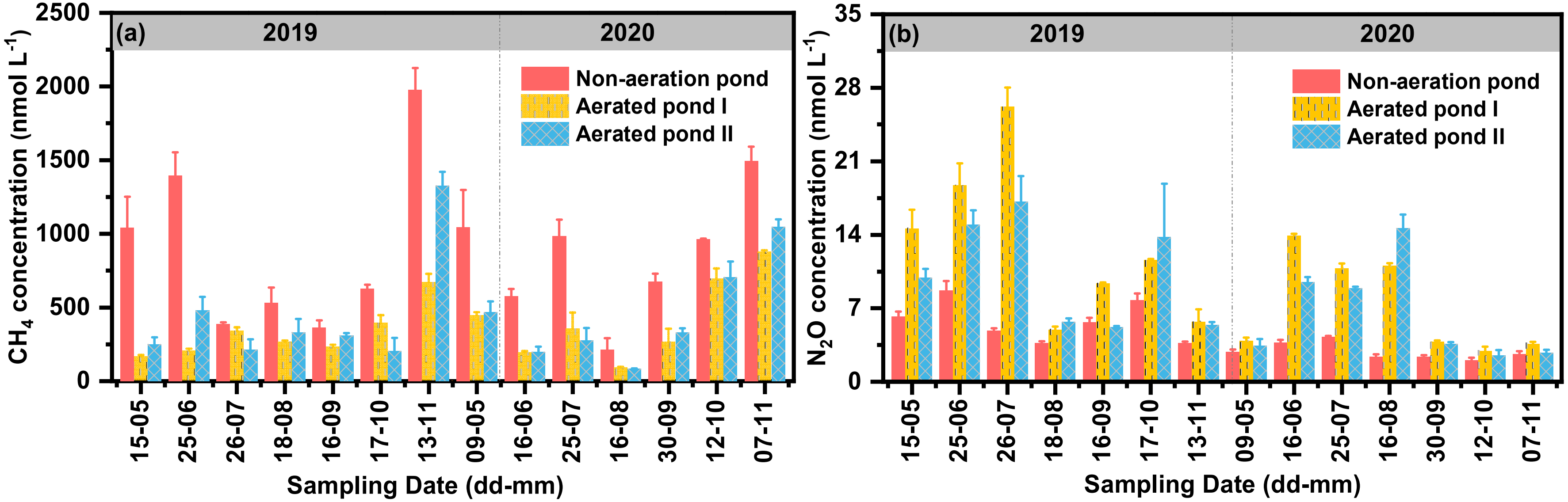

Figure 3. Dissolved CH_4 (a) and N_2O (b) concentrations in the aquaculture ponds during the farming period in 2019 and 2020. Bars represent mean ± 1SE (n = 3).

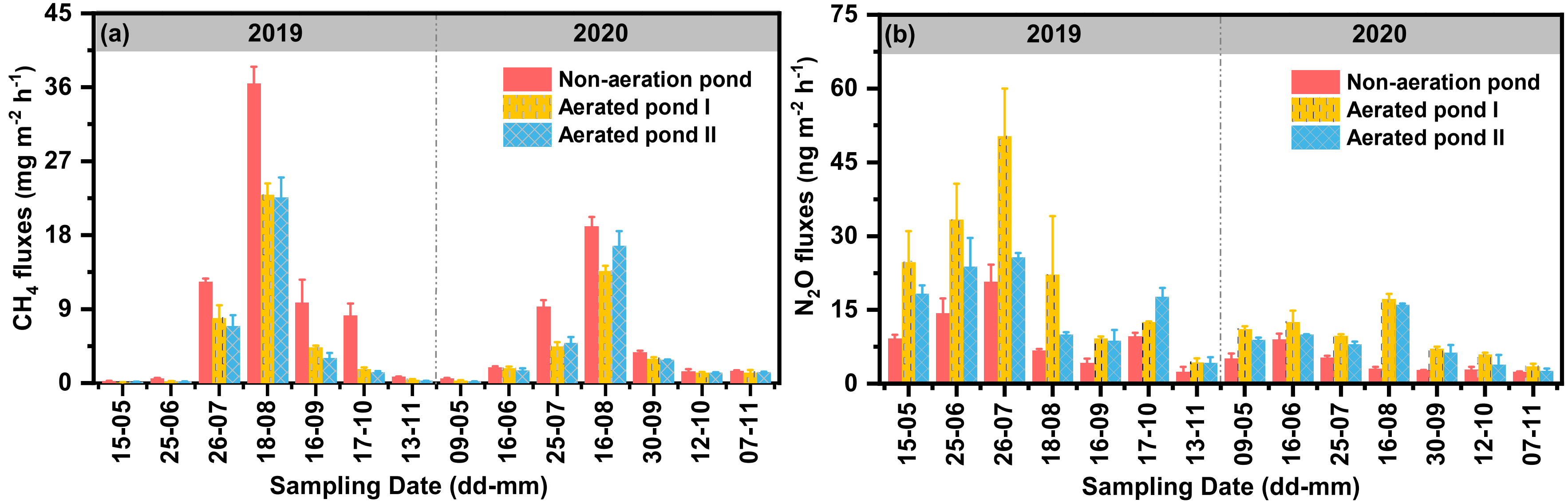

Figure 4. CH_4 (a) and N_2O (b) emission fluxes from the aquaculture ponds during the farming period in 2019 and 2020. Bars represent mean ± 1SE (n = 3).

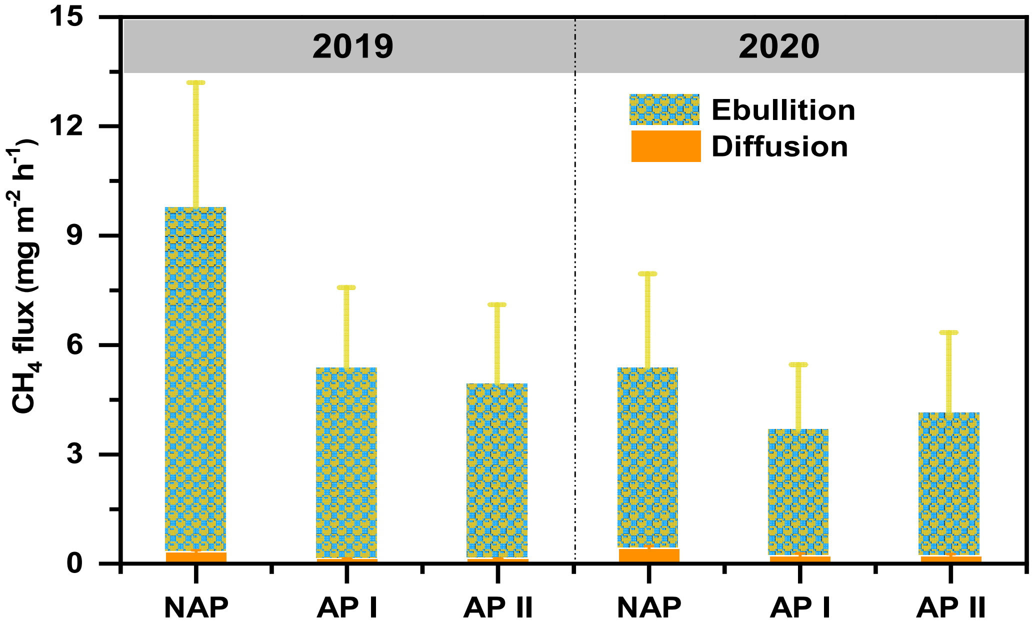

Figure 5. CH_4 ebullitive flux *vs* diffusive flux in the aquaculture ponds during the farming period in 2019 and 2020. NAP, AP I, and AP II represent non-aeration pond, aerated pond I and aerated pond II, respectively.

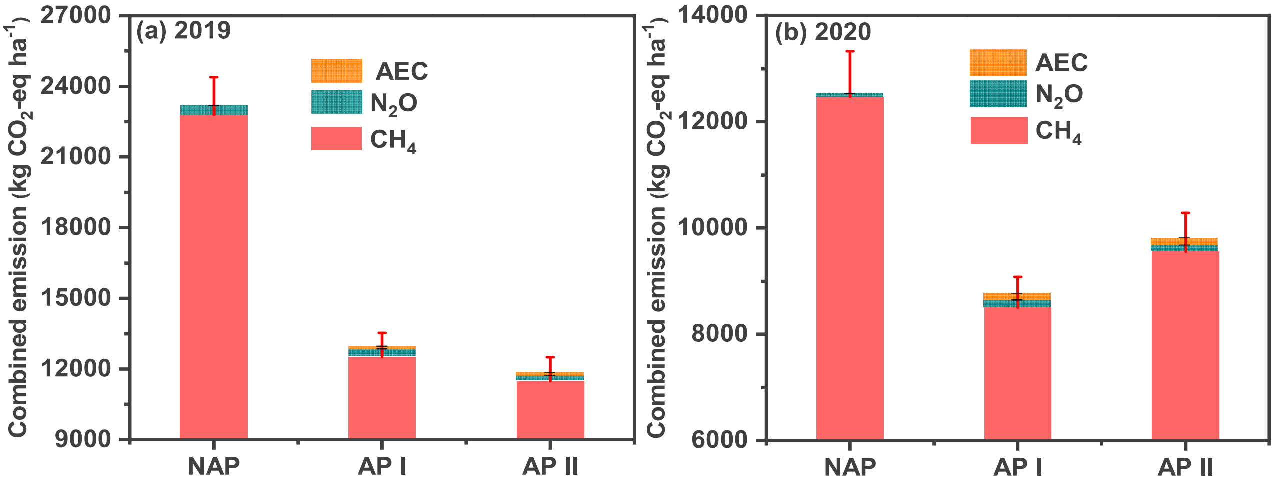

Figure 6. Combined CO_2-equivalent emissions from the aquaculture ponds during the farming period in 2019 (a) and 2020 (b). NAP represents non-aeration pond; AP I and AP II represent aerated pond I and II; AEC represent CO_2 emission from aerator's electricity consumption.

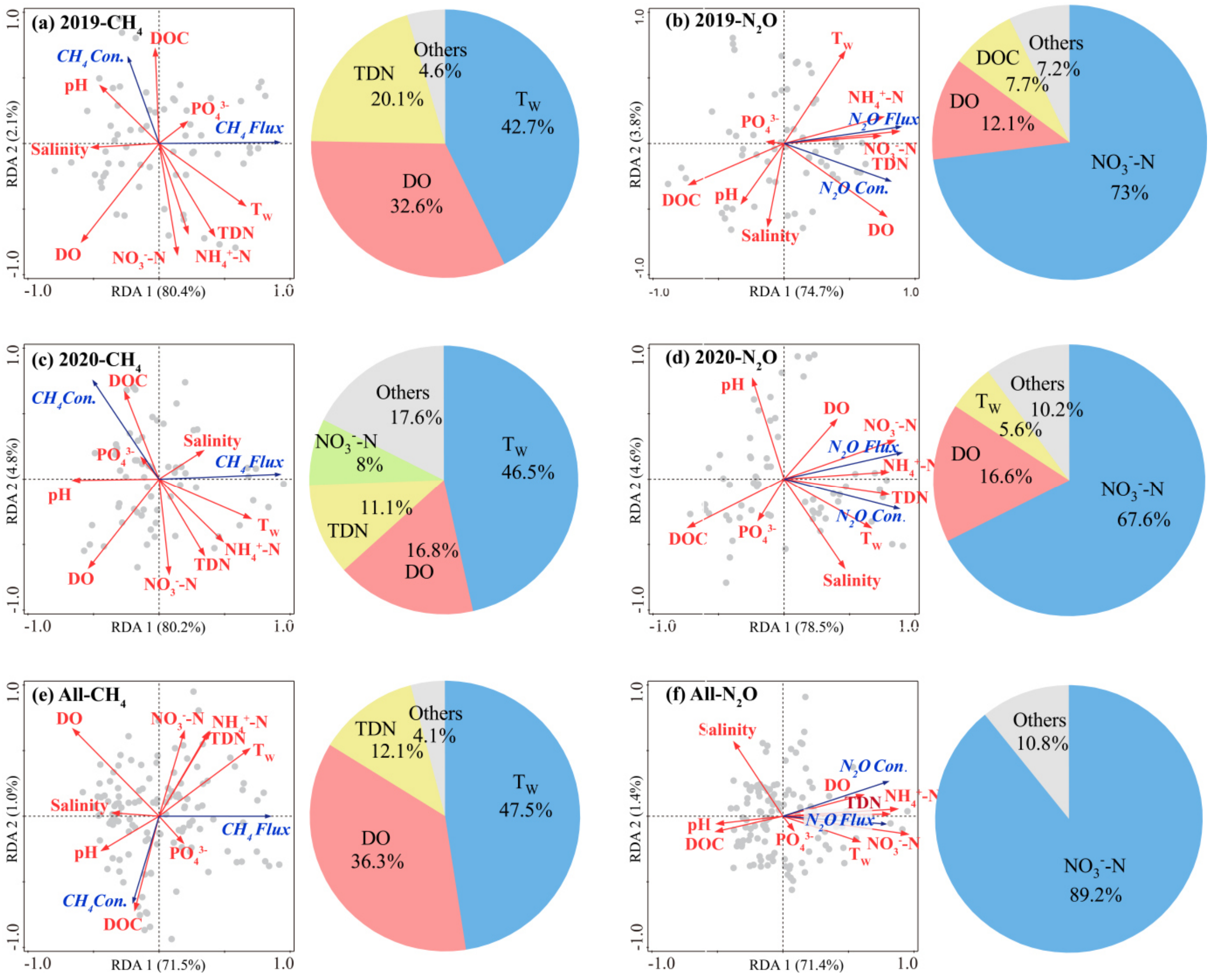

Figure 7. The redundancy analysis (RDA) biplots of the CH_4 (or N_2O) concentration and emission, and environmental parameters of the aquaculture ponds, showing the loadings of ancillary environmental parameters (arrows) and the scores of observations in two sampling years [2019 (a, b) and 2020 (c, d)] and in all sampling campaign all together (e, f). T_W, DO, DOC and TDN represent water temperature, dissolved oxygen, dissolved organic carbon and total dissolved organic nitrogen, respectively. The pie charts show the percentages of emission variance explained by the different parameters.

Supporting Information

Contrasting effects of aeration on methane (CH_4) and Nitrous oxide (N_2O) emissions from subtropical aquaculture ponds and implications for global warming mitigation

Ping Yang[a,b*], Kam W. Tang[c], Hong Yang[d,e], Chuan Tong[a,b], Linhai Zhang[a,b], Derrick Y. F. Lai[f], Yan Hong[a,b], Lishan Tan[f], Wanyi Zhu[a,b], Chen Tang[a,b]

[a]*School of Geographical Sciences, Fujian Normal University, Fuzhou 350007, P.R. China*

[b]*Key Laboratory of Humid Subtropical Eco-geographical Process of Ministry of Education, Fujian Normal University, Fuzhou 350007, P.R. China*

[c]*Department of Biosciences, Swansea University, Swansea SA2 8PP, U. K.*

[d]*Department of Geography and Environmental Science, University of Reading, Reading, UK*

[e]*College of Environmental Science and Engineering, Fujian Normal University, Fuzhou, 350007, China*

[f]*Department of Geography and Resource Management, The Chinese University of Hong Kong, Hong Kong, China*

***Correspondence to:**

Ping Yang (yangping528@sina.cn)

Telephone: 086-0591-87445659 Fax: 086-0591-83465397

Supporting Information Summary

No. of pages: 7 **No. of figures: 3** **No. of tables: 2**

Page S3: Figure S1 Boxplots of CH_4 (a) and N_2O (b) emission fluxes from non-aerated ponds and aerated ponds during the farming period in 2019 and 2020. Each box shows the quartiles and median, while the square and whiskers represent the mean and values within 1.5 times of the interquartile range, respectively. Different lowercase letters above the bars indicate significant differences (p<0.05) between ponds in each sampling year.

Page S4: Figure S2 Relationship between CH_4 (N_2O) emission flux and dissolved oxygen concentration (upper 20 cm water depth) in the aquaculture ponds during the farming period in 2019 and 2020, and in combined data.

Page S5: Figure S3 Relationships between NO_3^--N, NH_4^+-N, TDN concentrations and N_2O flux (upper 20 cm water depth) in the aquaculture ponds during the farming period in 2019 and 2020, and in combined data.

Page S6: Table S1 Summary of two-way ANOVAs (with sampling date specified as the random term) examining the effects of sampling ponds, sampling years and their interactions on the environmental variables in the surface water (upper 20 cm).

Page S7: Table S2 Pearson correlation coefficients between dissolved GHG concentrations, GHG emission fluxes and different environmental variables in the surface water (20-cm depth) in the aquaculture ponds.

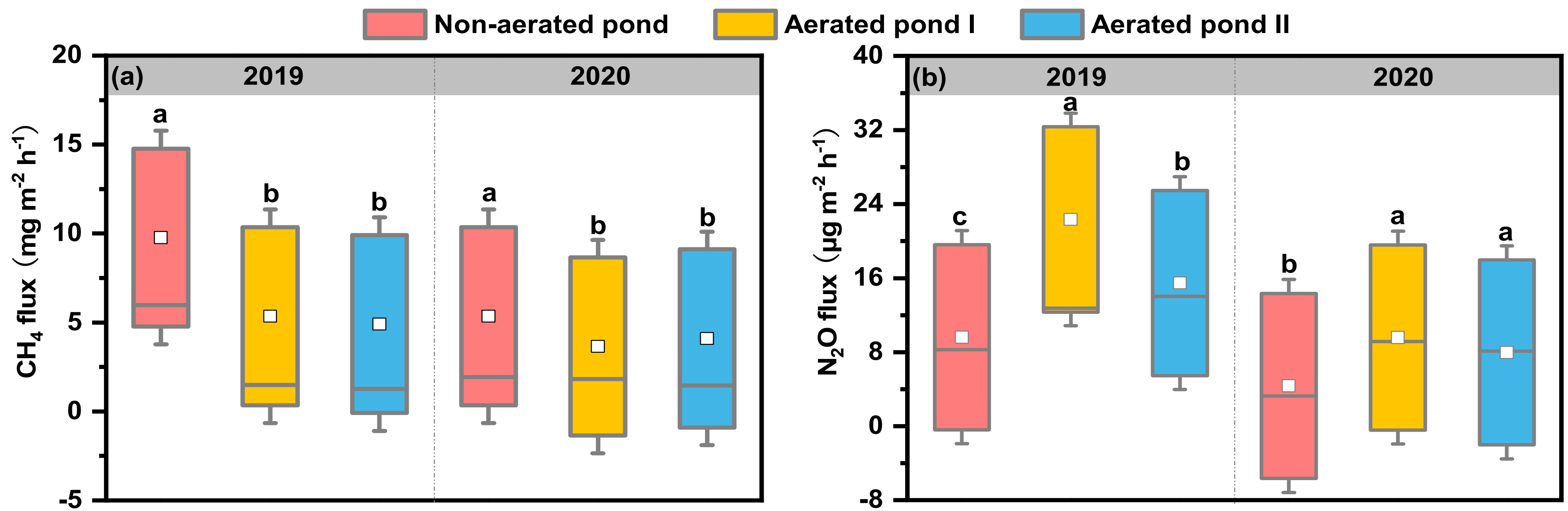

Figure S1. Boxplots of CH_4 (a) and N_2O (b) emission fluxes from non-aerated ponds and aerated ponds during the farming period in 2019 and 2020. Each box shows the quartiles and median, while the square and whiskers represent the mean and values within 1.5 times of the interquartile range, respectively. Different lowercase letters above the bars indicate significant differences (p<0.05) between ponds in each sampling year.

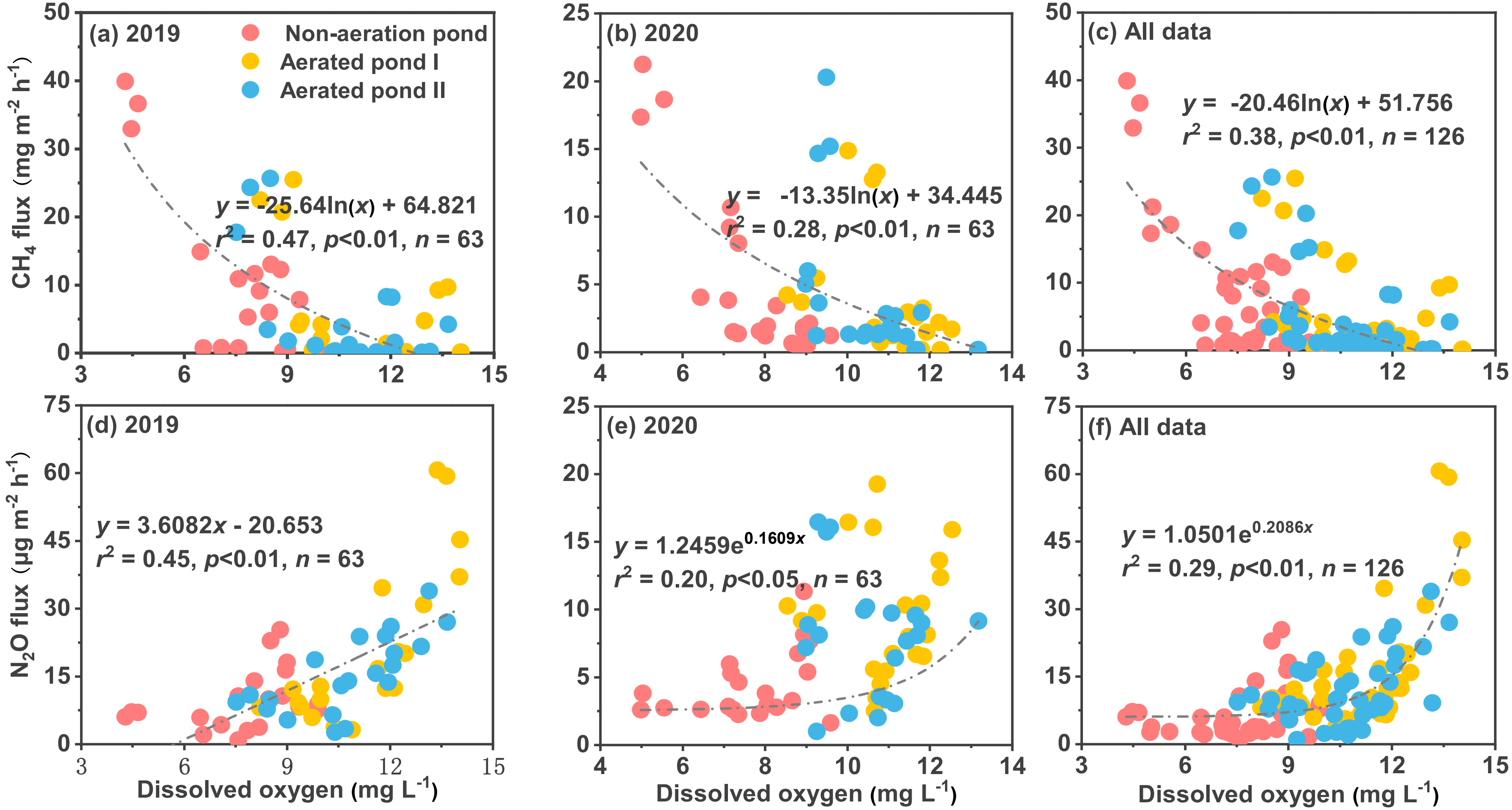

Figure S2. Relationship between CH_4 (N_2O) emission flux and dissolved oxygen concentration (upper 20 cm water depth) in the aquaculture ponds during the farming period in 2019 and 2020, and in combined data.

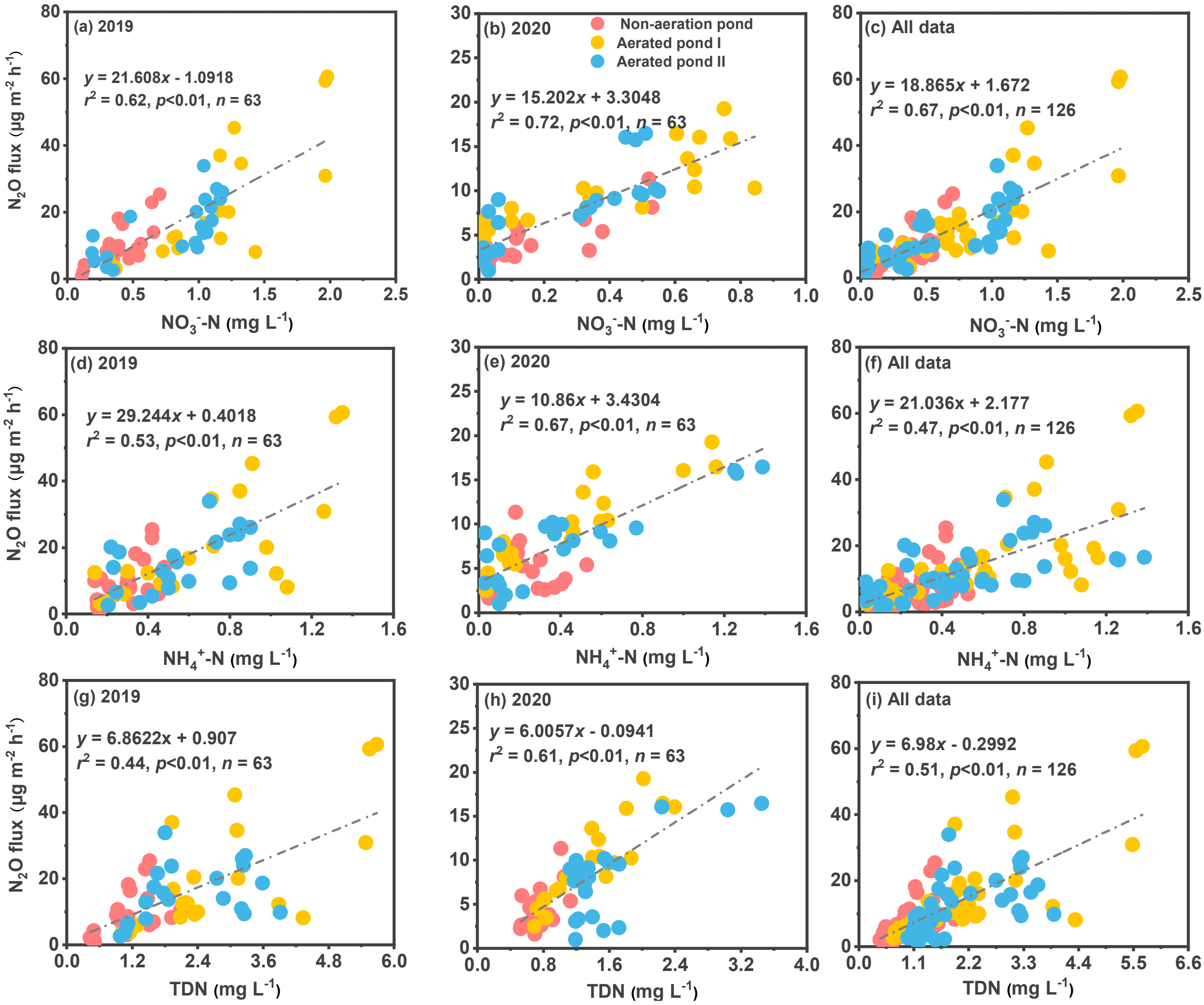

Figure S3. Relationships between NO_3^--N, NH_4^+-N, TDN concentrations and N_2O flux (upper 20 cm water depth) in the aquaculture ponds during the farming period in 2019 and 2020, and in combined data.

Table S1

Summary of two-way ANOVAs (with sampling date specified as the random term) examining the effects of sampling ponds, sampling years and their interactions on the environmental variables in the surface water (upper 20 cm).

	df	***T*W**		**pH**		**Salinity**		**DO**		**DOC**		**PO_4^{3-}**		**NO_3^--N**		**NH_4^+-N**		**TDN**	
		F	*p*	*F*	*p*	*F*	*p*	*F*	*p*	*F*	*p*	*F*	*p*	*F*	*p*	*F*	*p*	*F*	*p*
Sampling ponds	2	0.896	=0.434	0.620	=0.549	3.592	=0.060	147.11	**<0.001**	4.641	**<0.05**	0.992	=0.395	17.82	**<0.001**	10.490	=0.002	10.10	**=0.003**
Sampling years	1	5.907	=0.051	13.29	**=0.011**	31.02	**<0.001**	0.181	=0.686	2.484	=0.140	7.646	**=0.030**	28.72	**=0.002**	3.294	=0.200	9.105	**=0.023**
Sampling ponds × years	2	0.986	=0.401	0.817	=0.465	3.376	=0.069	0.023	=0.978	5.992	**=0.020**	0.634	=0.550	8.327	**=0.005**	1.482	=0.266	7.151	**=0.009**

T_W, water temperature; DO, dissolved oxygen; DOC, dissolved organic carbon; TDN, total dissolved organic nitrogen.

Table S2

Pearson correlation coefficients between dissolved GHG concentrations, GHG emission fluxes and different environmental variables in the surface water (20-cm depth) in the aquaculture ponds.

Environmental variables	Dissolved GHG concentration						GHG emission flux					
	CH_4			N_2O			CH_4			N_2O		
	2019	**2020**	**All data**	**2019**	**2020**	**All data**	**2019**	**2020**	**All data**	**2019**	**2020**	**All data**
Water temperature (T_W)	-0.480^{**}	-0.556^{**}	-0.474^{**}	**NS**	0.659^{**}	0.429^{**}	0.562^{**}	0.614^{**}	0.583^{**}	0.422^{**}	0.534^{**}	0.512^{**}
pH	0.381^{**}	0.301^{*}	0.258^{**}	**NS**	-0.404^{**}	-0.419^{**}	-0.362^{**}	-0.440^{**}	-0.370^{**}	-0.292^{*}	**NS**	-0.427^{**}
Salinity	**NS**	**NS**	**NS**	**NS**	0.558^{**}	-0.175^{*}	-0.419^{**}	**NS**	-0.300^{**}	**NS**	0.311^{*}	-0.352^{**}
Dissolved oxygen (DO)	-0.332^{**}	-0.264^{*}	-0.305^{**}	0.731^{**}	**NS**	0.530^{**}	-0.619^{**}	-0.491^{**}	-0.555^{**}	0.618^{**}	0.411^{**}	0.514^{**}
Dissolved organic carbon (DOC)	0.493^{**}	0.638^{**}	0.505^{**}	-0.438^{**}	-0.493^{**}	-0.438^{**}	0.265^{*}	0.554^{**}	0.326^{**}	-0.509^{**}	-0.644^{**}	-0.430^{**}
PO_4^{3-}	**NS**	**NS**	**NS**	**NS**	**NS**	**NS**	**NS**	**NS**	**NS**	**NS**	**NS**	**NS**
NO_3^--N	-0.478^{**}	-0.557^{**}	-0.498^{**}	0.612^{**}	0.707^{**}	0.659^{**}	**NS**	-0.273^{*}	**NS**	0.739^{**}	0.818^{**}	0.693^{**}
NH_4^+-N	-0.545^{**}	-0.576^{**}	-0.493^{**}	0.645^{**}	0.749^{**}	0.716^{**}	**NS**	0.353^{**}	0.315^{**}	0.680^{**}	0.782^{**}	0.743^{**}
Dissolved organic nitrogen (TDN)	-0.563^{**}	-0.560^{**}	-0.462^{**}	0.709^{**}	0.647^{**}	0.739^{**}	**NS**	**NS**	**NS**	0.793^{**}	0.838^{**}	0.824^{**}

The symbols * and ** denote significant correlations at $p < 0.05$ and $p < 0.01$, respectively. NS means non-significant relationship.